CHEMISTRY & BIODIVERSITY

Accepted Article

Title: Anti-inflammatory effect of Novel 7-substituted coumarin derivatives through inhibition of NF-κB signaling pathway

Authors: Chaoyu Mu, Mingfei Wu, and Zeng Li

To be cited as: *Chem. Biodiversity* 10.1002/cbdv.201800559

Link to VoR: http://dx.doi.org/10.1002/cbdv.201800559

10.1002/cbdv.201800559

Anti-inflammatory effect of novel 7-substituted coumarin derivatives through inhibition of NF-κB signaling pathway

Chaoyu Mu [a, b], Mingfei Wu [a] and Zeng Li [a, *]

[a] *School of Pharmacy, Anhui Medical University, Hefei 230032 China.*
[b] *Department of Clinical Laboratory, Huaibei Miner's General Hospital, Huaibei 235000 China.*

***** Corresponding author.
E-mail address: lizeng@ahmu.edu.cn

10.1002/cbdv.201800559

Abstract: A series of novel 7-substituted coumarin derivatives was synthesized and evaluated. Biological screening results obtained by the evaluation of the compounds' inhibition against LPS-induced IL-6 and TNF-α release in RAW 264.7 cells indicated that most compounds exhibited potent anti-inflammatory activity. Among them, compound **2d** showed the best activity. The potential targets of title compound **2d** were reverse screened with the molecular modeling software-Discovery Studio 2017 R2. Screening and molecule docking results showed that **2d** may bind the active site (NLS Polypeptide) of NF-κB p65, and this binding affinity was confirmed by surface plasmon resonance (SPR)analysis. Furthermore, western blot assay showed that **2d** remarkably blocked the NF-κB signaling pathway in vitro. Collectively, all these findings suggested that compound **2d** might be a promising lead compound worthy of further pursuit.

Keywords: coumarin derivative, anti-inflammatory, 2d, reverse screen, NF-κB

10.1002/cbdv.201800559

Introduction

Inflammation is the response of living tissues to cellular injury and involves innate and adaptive immunity [1]. The purpose of inflammation is to localize and eliminate causative agents, limit tissue injury, and restore tissue to normality. Thus, inflammation is one of the most common and important basic pathological processes involved in infectious diseases [2], tissue damage [3], initiation and promotion of cancer [4], and development of atherosclerosis [5]. Classic anti-inflammatory drugs can be divided into two types: steroidal anti-inflammatory drugs (SAIDs) and non-SAIDs (NSAIDs). The former is a type of hormone and have many physiological effects. When administered for inflammatory diseases, they may cause many side effects [6]. The latter inhibit COX-1 and COX-2 simultaneously; however, they may cause adverse gastric effects that lead to patient intolerance [7]. Therefore, to aim at the mechanisms of inflammation, exploring and developing new anti-inflammatory drugs is important.

Coumarins, a class of natural organic compounds that contains a benzopyrone core, have multiple biological activities, such as antimicrobial, anticancer, anti-inflammation, antitubercular, and antioxidant activity; inhibition of platelet aggregation; and cardiovascular protection [8]. The anti-inflammatory properties of coumarins are attributed to their inhibition of the production of TNF-α and other pro-inflammatory cytokines by activated macrophages [9]. Moreover, various coumarin-related derivatives serve as inhibitors of the lipoxygenase and cyclooxygenase pathways of arachidonate metabolism [10-11]. Given its favorable anti-inflammatory activity, a coumarin framework has been used for chemical modification for identifying novel derivatives with improved pharmacological or pharmacokinetic profiles.

Substituted aniline, benzylamine, and phenethylamine moieties belong to an important class of organic compounds that is widely used in medicinal chemistry. These substituents are often present in anti-inflammatory drug constructs. Thus, we synthesized some coumarin derivatives hybridized with substituted aniline or benzene methylamine moieties as possible anti-inflammatory agents (*Scheme 1*). In this study,

 10.1002/cbdv.201800559

we selected LPS-stimulated RAW264.7 cells as a cellular model to evaluate the anti-inflammatory activity of target compounds.

Results and discussion

Chemistry

Coumarin derivatives (**2a–2k**) were synthesized from two steps, as described in *Scheme 1*. Intermediate 1 was obtained under relatively mild conditions by condensing 7-hydroxycoumarin with ethyl bromoacetate in the presence of K_2CO_3 as base in DMF at 60 °C. Reacting the intermediate **1** with the substituted aniline or benzene methylamine in ethanol at 78 °C afforded the target compounds **2a–2k**.

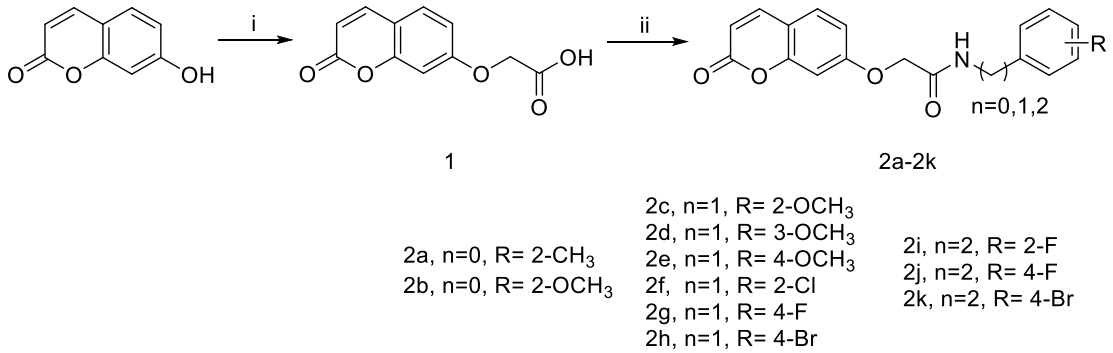

Scheme 1. Synthesis route of coumarin derivatives **2a-2k**. (i) Ethyl Bromoacetate, K_2CO_3, acetone, 12 h, rt; 5% sodium hydroxide, 2 h, rt; (ii) Aniline or benzene methylamine, CH_2Cl_2, 2 h, rt.

MTT assay

MTT was first used to screen the influences of coumarin derivatives on the proliferation of LPS-activated RAW264.7 cells. The results (*Table s1, Figure 1*) indicated that stimulator LPS (0.5–1 μg/mL) and all coumarin derivatives (1–10 μM) in the presence of LPS (1 μg/mL) showed little toxic effects on RAW 264.7 cells. Even at high concentrations, LPS (2 μg/mL) and several coumarin derivatives (**2c**, **2e**, **2f**, **2i**, and **2k** at 100 μM) presented certain toxic effects. Thus, we further chose the concentrations of 1 μg/mL LPS and 10 μM coumarin derivatives in the subsequent

10.1002/cbdv.201800559

analyses.

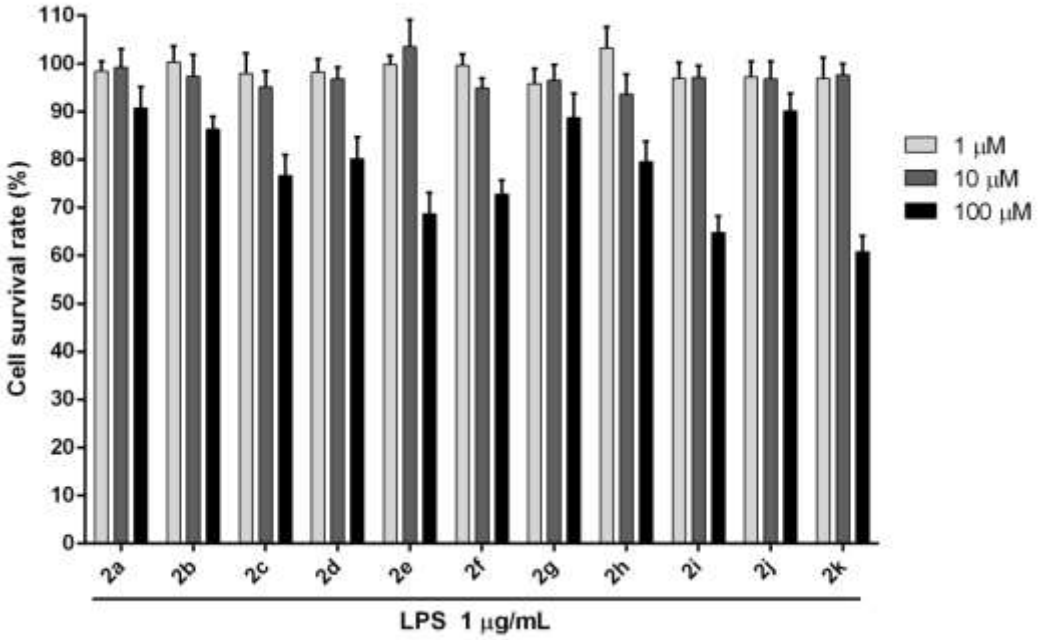

Figure 1. Effects of indicated concentrations of coumarin derivatives on viability of LPS-activated RAW264.7 cells. All measurements were obtained in triplicate. Values are presented as mean ± SD.

The detection of key pro-inflammatory cytokine

The detection of key pro-inflammatory cytokine induced by LPS-activated RAW 264.7 cells is an essential step for an anti-inflammatory agent [12]. The anti-inflammatory activity of coumarin derivatives on the pro-inflammatory mediators IL-6 and TNF-α release of LPS-activated RAW 264.7 cells is illustrated in *Figure 2*. Compared with the LPS group, the levels of TNF-α and IL-6 were statistically significantly lower in LPS-stimulated macrophages of most coumarin derivatives (such as **2c**, **2d**, and **2e**). Among them, compound **2d** was the most potent coumarin derivative (inhibition rate up to -50% compared with LPS). Preliminary SARs showed that substituent R substantially affected the anti-inflammatory activity and the methoxy group was better than that of halogen substitution. The methoxy group at 3-position was also important. These results indicated that coumarin derivatives could markedly inhibit the LPS-induced release of various proinflammatory cytokines with

10.1002/cbdv.201800559

potential anti-inflammatory activity.

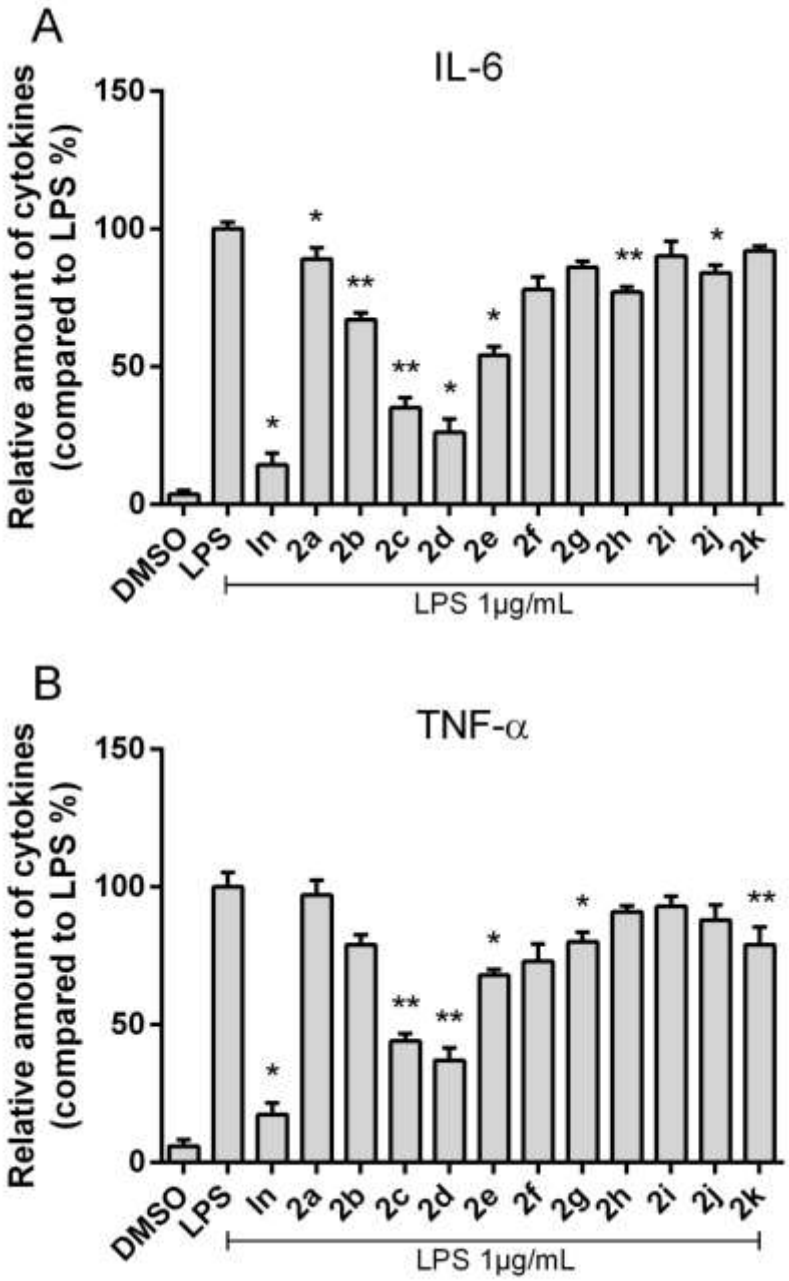

Figure 2. Effects of coumarin derivatives (10 μM) on IL-6 and TNF-α production in LPS-activated RAW264.7 cells. All measurements were obtained in triplicate. Values are presented as mean ± SD. In=Indomethacin (10 μM). Statistical significance compared with the LPS group was indicated, *p <0.05, **p <0.01.

Reverse virtual screening and Molecule docking

Computer-aided simulation on the construction of a pharmacophore model based

10.1002/cbdv.201800559

on the function of the active ligand-building pharmacophore model and receptor-ligand crystal complex can shorten experiments remarkably [13]. For this research, we used reverse virtual screening to validate that coumarin derivative **2d** had a good binding relationship with NF-κB p65 (PDB 1MY5) [14] (*Figure 3*). Thus, NF-κB was considered a possible target of 2d. Further analysis of the results was conducted by molecule docking using C-DOCKER in Discovery Studio 2017 R2. The protein crystal structure of NF-κB p65 (PDB 1MY5) was used. As shown in *Figure 4*, a typical docking pose demonstrated that compound **2d** could bind to the active site (NLS Polypeptide) of p65. Two hydrogen bonds interacted between 2d and p65 NLS Polypeptide: one was between the -O- group of the lactone and residue of ASP293, and the other was between the -NH- group with ASP293. The coumarin core of 2d was inserted into the active site deeply. **2d** also exhibited the π-π stacking interaction between the aromatic ring and the residue of LEU207 and PRO260. Additionally, certain weak interactions, including pi-alkyl, carbon-hydrogen bonds, and van der Waals, contributed to the binding affinity of **2d** with NF-κB p65.

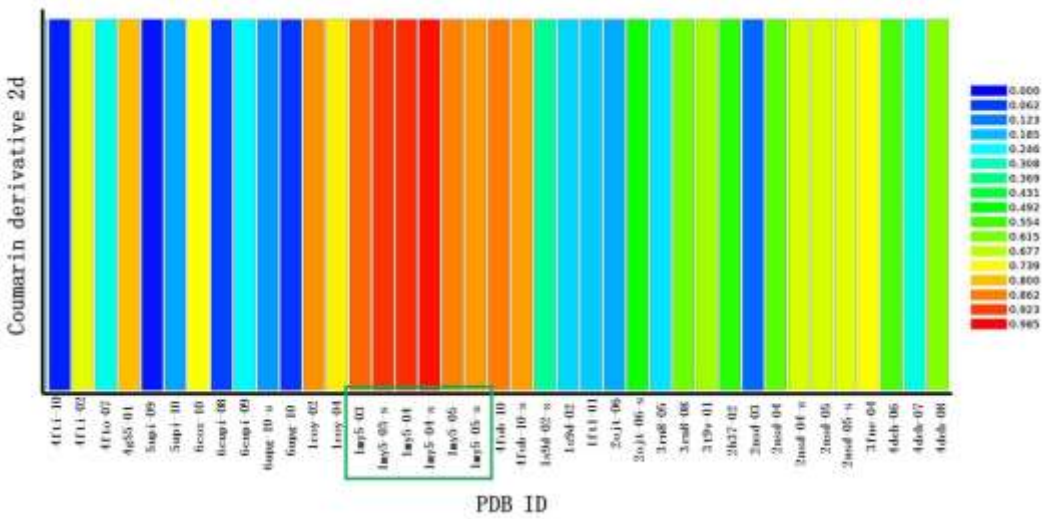

Figure 3. Profiling of the predicted protein targets of **2d** via Discovery Studio 2017 R2. The Y-axis represents the compound **2d**, and the X-axis indicates the predicted pharmacophore models (pharmacological targets). The color from blue to red represents a higher fit value and a better fit.

10.1002/cbdv.201800559

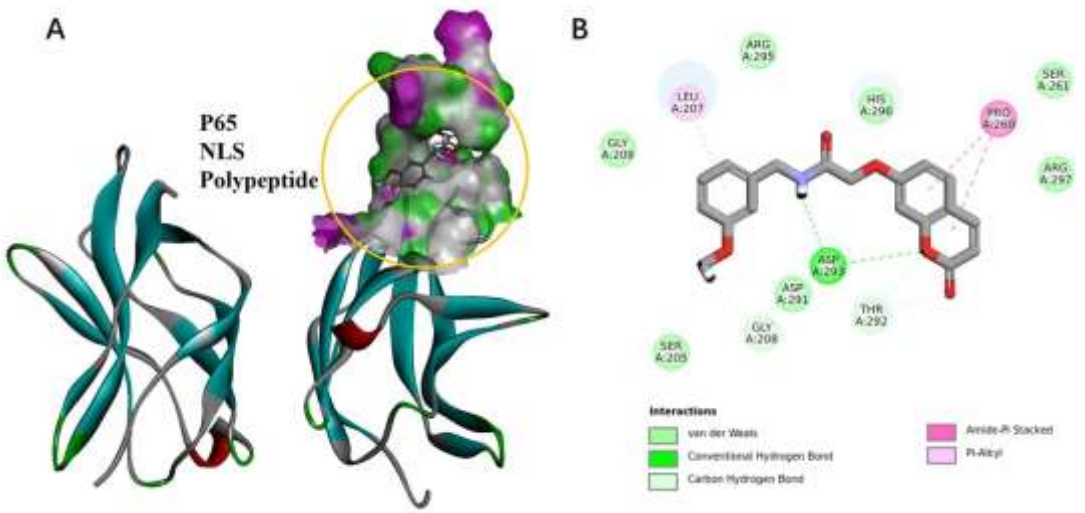

Figure 4. (A) 3D model of the interaction between compound **2d** with the active site of NF-κB p65. (B) 2D model of the interaction between compound **2d** with the active site of NF-κB p65.

Binding affinity of the compound 2d to NF-κB p65

SPR is a useful technique to monitor molecular reactions in real time, which has been applied to investigate the interactions between small molecule and proteins. To confirm the binding affinity of coumarin derivative **2d** with NF-κB p65, SPR experiments was performed. *Figure 5* shows the SPR sensorgrams of **2d** binding to the immobilized NF-κB p65 at the concentration of 12.5, 25, 50, 100, 200 and 400 nM. The association of **2d** with NF-κB p65 was evaluated using the equilibrium dissociation constant (KD) by fitting the sensogram with a 1:1 (Langmuir) binding fit model. The results showed that **2d** had a high binding affinity toward NF-κB p65 with a KD value of 2.83×10^{-7} M.

10.1002/cbdv.201800559

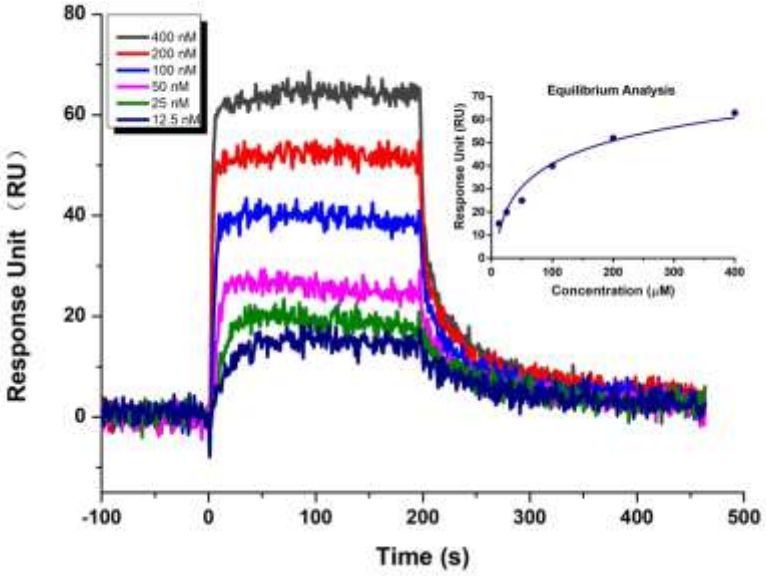

Figure 5. SPR sensograms for coumarin derivative **2d** binding to the immobilized NF-κB p65. Concentration range: 400, 200, 100, 50, 25, and 12.5 nM for the curves from the bottom curve upward. Binding plots used to determine the KD value for **2d** with NF-κB p65 in the inner panel.

Western blot assay

The NF-κB signaling pathway is important in the critical juncture of inflammation [15]. NF-κB is often located in the cytoplasm in non-activated cells as a polymer that consists of p50, p65, and IkB proteins. In response to an activation signal, NF-κB becomes phosphorylated and degraded [16]. Furthermore, various pro-inflammatory agents, including interleukins, cytokines, chemokines, iNOS, and COX-2, are promoted in transcription [17]. To understand the effect of compound **2d** on LPS-stimulated NF-κB signaling pathway, the expression of the relative protein of p65, phospho p65, COX-2, and INOS were checked by western blot assay. As shown in *Figure 6*, the title compound **2d** remarkably decreased the phosphorylation of p65, and certain downstream signaling molecules, such as iNOS and COX-2, were also inhibited. Combined with the reverse virtual screening results, these findings indicated that **2d** is a potent inhibitor of NF-κB activity that exhibits anti-inflammatory activity.

10.1002/cbdv.201800559

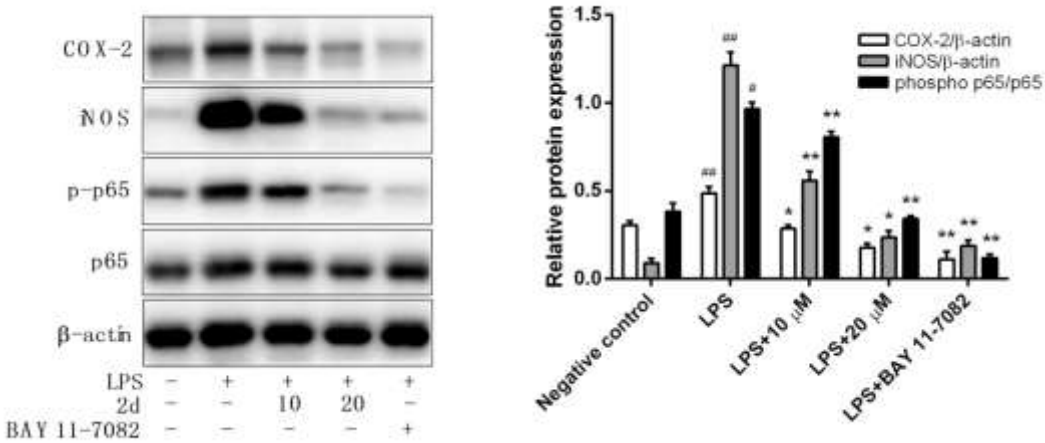

Figure 6. Coumarin derivative **2d** inhibited the activation of NF-κB signaling pathway in LPS-activated RAW264.7 cells. Western blot analysis (A) and quantitative data of protein (B) BAY11-7082 was used as the positive control. $^{\#}p < 0.05$, $^{\#\#}p < 0.01$ compared with the negative control group. $^{*}p < 0.05$, $^{**}p < 0.01$ compared with the LPS group. Values are presented as mean ± SD.

Conclusion

In summary, to identify original, effective lead compounds that can serve as an anti-inflammatory agent, a series of 7-substituted coumarin derivatives were synthesized and evaluated. Most compounds exhibited potent anti-inflammatory activity, especially compound **2d**. The preliminary mechanism study found that 2d may bind the active site (NLS Polypeptide) of NF-κB p65 to block the NF-κB signaling pathway. The results were confirmed by SPR and Western blot assay. The data presented in this work indicated that coumarin derivative **2d**'s anti-inflammatory role may be partly due to its inhibitory effect on the NF-κB signaling pathway. Additional studies and tests on its mechanism of anti-inflammatory activity are underway.

Experimental Section

Chemistry

 10.1002/cbdv.201800559

All required chemicals and solvents were purchased from Sigma-Aldrich (Munich, Germany). Melting points were determined on a XT4MP apparatus (Taike Corp., Beijing, China), and are uncorrected. ^{1}H-NMR spectra are recorded using TMS as the internal standard in $CDCl_3$ solutions on a Bruker 400 MHz instrument (Bruker, Karlsruhe, Germany). High-resolution electron impact mass spectra (HRMS) were recorded under electron impact (70 eV) condition using a Micro Mass GCT CA 055 instrument.

Synthesis of intermediate 1

A mixture of 7- hydroxycoumarin (6.17 mmol), ethyl bromoacetate (9.15 mmol) and K_2CO_3 (4.69 g, 33.91 mmol) in acetone (30 mL) was heated under reflux for 12h. After cooling to room temperature, the mixture was evaporated to dryness. The residue was dissolved in ethanol (50 mL) was refluxed with 5% sodium hydroxide (5 mL) for 2 h. The mixture was evaporated to dryness, then dissolved into water and acidified with HCl (6 M). A white precipitate was formed, filtered, and washed with cool water, dried and recrystallized from ethanol to afford **1**, yield 67%. m.p. 210-211℃; ^{1}H NMR (400 MHz, DMSO) δ 7.99 (d, *J* = 9.5 Hz, 1H), 7.70 – 7.56 (m, 1H), 7.02 – 6.90 (m, 2H), 6.29 (d, *J* = 9.5 Hz, 1H), 4.77 (s, 2H). HRMS (ESI) *m*/*z*: calcd for $C_{11}H_8O_5$ $[M+H]^+$: 221.0444, found 221.0448.

General procedures for the preparation of target compounds 2a-2k

A suspension compound **1** (0.945mmol) in dichloromethane (20 mL) was stirred at room temperature with oxalyl chloride (1.42mmol), DMF (1mL) for 2 h. After cooling, the mixture was evaporated to dryness and the residue dissolved in dichloromethane (20 mL). The solution was refluxed with substituted aniline, benzylamine or phenethylamine (1.134 mmol) for 5 h. Then the solvent was poured into water and extracted with dichloromethane (50 mL × 3). The solution was dried over anhydrous Na_2SO_4 and concentrated. The residues were purified by flash chromatography with mineral ether/ethyl acetate (2:1, *v*/*v*) elution.

2-((2-oxo-2H-chromen-7-yl)oxy)-N-(m-tolyl)acetamide (2a)

White solid (63 % yield); m.p. 187-188 ℃; ^{1}H NMR (400 MHz, $CDCl_3$) δ 8.13 (s, 1H), 7.66 (d, *J* = 9.5 Hz, 1H), 7.45 (dd, *J* = 11.4, 8.4 Hz, 2H), 7.38 (d, *J* = 8.1 Hz, 1H), 7.24 (d, *J* = 7.9 Hz, 1H), 7.03 – 6.91 (m, 3H), 6.32 (d, *J* = 9.5 Hz, 1H), 4.67 (s, 2H),

 10.1002/cbdv.201800559

2.36 (s, 3H). HRMS (ESI) *m/z*: calcd for $C_{18}H_{15}NO_4$ $[M+H]^+$: 310.1074, found 310.1078.

N-(2-methoxyphenyl)-2-((2-oxo-2H-chromen-7-yl)oxy)acetamide (2b)

White solid (72 % yield); m.p. 191-193 ℃; ^{1}H NMR (400 MHz, $CDCl_3$) δ 8.87 (s, 1H), 8.38 (dd, *J* = 8.0, 1.5 Hz, 1H), 7.66 (d, *J* = 9.5 Hz, 1H), 7.46 (d, *J* = 9.3 Hz, 1H), 7.10 (td, *J* = 7.9, 1.6 Hz, 1H), 6.99 (td, *J* = 7.8, 1.2 Hz, 1H), 6.97 – 6.93 (m, 2H), 6.91 (dd, *J* = 8.1, 1.2 Hz, 1H), 6.32 (d, *J* = 9.5 Hz, 1H), 4.69 (s, 2H), 3.90 (s, 3H). HRMS (ESI) *m/z*: calcd for $C_{18}H_{15}NO_5$ $[M+H]^+$: 326.1023, found 326.1026.

N-(2-methoxybenzyl)-2-((2-oxo-2H-chromen-7-yl)oxy)acetamide (2c)

White solid (54 % yield); m.p. 182-183 ℃; ^{1}H NMR (400 MHz, $CDCl_3$) 1H NMR (400 MHz, CDCl3) δ 7.64 (d, J = 9.5 Hz, 1H), 7.41 (d, J = 8.1 Hz, 1H), 7.25 – 7.20 (m, 2H), 6.90 – 6.82 (m, 4H), 6.75 (s, 1H), 6.30 (d, J = 9.5 Hz, 1H), 4.59 (s, 2H), 4.49 (d, J = 5.8 Hz, 2H), 3.80 (s, 3H). HRMS (ESI) *m/z*: calcd for $C_{19}H_{17}NO_5$ $[M+H]^+$: 340.1179, found 340.1182.

N-(3-methoxybenzyl)-2-((2-oxo-2H-chromen-7-yl)oxy)acetamide (2d)

White solid (66 % yield); m.p. 179-180 ℃; ^{1}H NMR (400 MHz, $CDCl_3$) δ 7.64 (d, *J* = 9.5 Hz, 1H), 7.42 – 7.37 (m, 1H), 7.31 – 7.23 (m, 1H), 6.89 – 6.81 (m, 6H), 6.30 (d, *J* = 9.5 Hz, 1H), 4.59 (s, 2H), 4.54 (d, *J* = 6.1 Hz, 2H), 3.83 (s, 3H). HRMS (ESI) *m/z*: calcd for $C_{19}H_{17}NO_5$ $[M+H]^+$: 340.1179, found 340.1175.

N-(4-methoxybenzyl)-2-((2-oxo-2H-chromen-7-yl)oxy)acetamide (2e)

White solid (47 % yield); m.p. 191-193 ℃; ^{1}H NMR (400 MHz, $CDCl_3$) δ 7.64 (d, J = 9.5 Hz, 1H), 7.41 (d, J = 8.7 Hz, 1H), 7.25 – 7.18 (m, 2H), 6.94 – 6.82 (m, 4H), 6.75 (s, 1H), 6.29 (d, J = 9.5 Hz, 1H), 4.59 (s, 2H), 4.49 (d, J = 5.9 Hz, 2H), 3.80 (s, 3H). HRMS (ESI) *m/z*: calcd for $C_{19}H_{17}NO_5$ $[M+H]^+$: 340.1179, found 340.1175.

N-(2-chlorobenzyl)-2-((2-oxo-2H-chromen-7-yl)oxy)acetamide (2f)

White solid (51 % yield); m.p. 186-187 ℃; ^{1}H NMR (400 MHz, $CDCl_3$) δ 7.64 (d, J = 9.5 Hz, 1H), 7.47 – 7.32 (m, 3H), 7.25 (dd, J = 5.8, 3.5 Hz, 2H), 7.00 (s, 1H), 6.87 (dd, J = 8.6, 2.5 Hz, 1H), 6.83 (d, J = 2.4 Hz, 1H), 6.30 (d, J = 9.5 Hz, 1H), 4.64 (d, J = 6.2 Hz, 2H), 4.59 (s, 2H). HRMS (ESI) *m/z*: calcd for $C_{18}H_{14}ClNO_4$ $[M+H]^+$: 344.0684, found 344.0687.

 10.1002/cbdv.201800559

N-(4-fluorobenzyl)-2-((2-oxo-2H-chromen-7-yl)oxy)acetamide (2g)

White solid (67 % yield); m.p. 179-180 °C; ^{1}H NMR (400 MHz, $CDCl_3$) δ 7.64 (d, *J* = 9.5 Hz, 1H), 7.42 (d, *J* = 9.1 Hz, 1H), 7.30 – 7.27 (m, 2H), 7.03 (dd, *J* = 11.9, 5.4 Hz, 2H), 6.91 – 6.79 (m, 3H), 6.30 (d, *J* = 9.5 Hz, 1H), 4.60 (s, 2H), 4.53 (d, *J* = 6.0 Hz, 2H). HRMS (ESI) *m*/*z*: calcd for $C_{18}H_{15}FNO_4$ $[M+H]^+$: 328.0980, found 328.0977.

N-(4-bromobenzyl)-2-((2-oxo-2H-chromen-7-yl)oxy)acetamide (2h)

White solid (71 % yield); m.p. 193-194 °C; ^{1}H NMR (400 MHz, $CDCl_3$) δ 7.64 (d, J = 9.5 Hz, 1H), 7.51 – 7.44 (m, 2H), 7.42 (d, J = 9.3 Hz, 1H), 7.18 (d, J = 8.5 Hz, 2H), 6.86 (q, J = 2.5 Hz, 3H), 6.30 (d, J = 9.5 Hz, 1H), 4.60 (s, 2H), 4.51 (d, J = 6.1 Hz, 2H). HRMS (ESI) *m*/*z*: calcd for $C_{18}H_{14}BrNO_4$ $[M+H]^+$: 388.0179, found 388.0179.

N-(2-fluorophenethyl)-2-((2-oxo-2H-chromen-7-yl)oxy)acetamide (2i)

White solid (68 % yield); m.p. 195-196 °C; ^{1}H NMR (400 MHz, $CDCl_3$) δ 7.65 (d, *J* = 9.5 Hz, 1H), 7.42 (d, *J* = 8.4 Hz, 1H), 7.19 (dt, *J* = 17.0, 3.6 Hz, 2H), 7.10 – 6.97 (m, 2H), 6.82 (dt, *J* = 4.1, 2.4 Hz, 2H), 6.60 (s, 1H), 6.31 (d, *J* = 9.5 Hz, 1H), 4.52 (s, 2H), 3.63 (q, *J* = 6.7 Hz, 2H), 2.92 (t, *J* = 6.8 Hz, 2H). HRMS (ESI) *m*/*z*: calcd for $C_{19}H_{16}FNO_4$ $[M+H]^+$: 342.1136, found 342.1138.

N-(4-fluorophenethyl)-2-((2-oxo-2H-chromen-7-yl)oxy)acetamide (2j)

White solid (77 % yield); m.p. 192-193 °C; ^{1}H NMR (400 MHz, $CDCl_3$) δ 7.65 (d, *J* = 9.5 Hz, 1H), 7.41 (d, *J* = 8.3 Hz, 1H), 7.25 (d, *J* = 7.5 Hz, 2H), 7.09 (d, *J* = 8.4 Hz, 2H), 6.79 (dd, *J* = 11.1, 2.6 Hz, 2H), 6.49 (s, 1H), 6.31 (d, *J* = 9.5 Hz, 1H), 4.53 (s, 2H), 3.61 (dd, *J* = 13.2, 6.9 Hz, 2H), 2.84 (t, *J* = 7.0 Hz, 2H). HRMS (ESI) *m*/*z*: calcd for $C_{19}H_{16}FNO_4$ $[M+H]^+$: 342.1136, found 342.1140.

N-(4-bromophenethyl)-2-((2-oxo-2H-chromen-7-yl)oxy)acetamide (2k)

White solid (79 % yield); m.p. 196-197 °C; ^{1}H NMR (400 MHz, $CDCl_3$) δ 7.66 (d, *J* = 9.5 Hz, 1H), 7.40 (dd, *J* = 10.9, 8.4 Hz, 3H), 7.04 (d, *J* = 8.2 Hz, 2H), 6.79 (dd, *J* = 13.3, 2.2 Hz, 2H), 6.48 (s, 1H), 6.32 (d, *J* = 9.5 Hz, 1H), 4.53 (s, 2H), 3.60 (q, *J* = 6.8 Hz, 2H), 2.82 (t, *J* = 7.0 Hz, 2H). HRMS (ESI) *m*/*z*: calcd for $C_{19}H_{16}BrNO_4$ $[M+H]^+$: 402.0335, found 402.0331.

10.1002/cbdv.201800559

Cell culture

Mouse macrophage cell line RAW 264.7 were cultured in cell culture bottles in DMEM medium (Hyclone, USA) supplemented with 10% fetal bovine serum（FBS, sijiqing, Hangzhou, Zhejiang, China. All cell cultures were maintained at 37℃ in a humidified incubator at an atmosphere of 5% CO_2. All of the operations provided by approved guidelines and regulations.

3-(4,5-Dimethylthiazol-2-yl)-2,5-diphenyltetrazolium bromide (MTT) assay

Proliferation of cells was measured using MTT assay. The cells were seeded on 96-well culture plates, until the cells reached 70%-80% confluency, and then treated with LPS (0, 0.5, 1, 2 μg/mL) for 24 h. Repeat these steps, cells were pretreated with coumarin derivatives (1 μM, 10 μM and 100 μM) for 24 h after stimulation with 1 μg/ml LPS for 24 h. MTT solution (5 mg/ml, Invitrogen) was added to each well and the resulting mixture was incubated for 4 h at 37 °C. Finally, removing the supernatant, 150μl DMSO was added to each well, and the plates were read at 490 nm wavelength. All measurement were obtained in triplicate.

The detection of pro-inflammatory cytokine IL-6 and TNF-α

The RAW 264.7 cells were stimulated with LPS (1 μg/mL) for 24 h and then treated with indomethacin, coumarin derivatives (10 μM) for 24 h. IL-6 and TNF-α levels in the culture media were measured by ELISA and were normalized by the total protein. The IL-6 and TNF-α ELISA Kit were purchased from Sigma-Aldrich Co (St. Louis, MO, USA). All measurement were obtained in triplicate.

Reverse virtual screening and Molecular docking

To understand the potential interactions between the tested drug and selected protein, reverse direction finding were performed using Discovery Studio 2017 R2 (DS) in this study. The ligand structure was drawn by using the ChemDraw2010 program. Ligand structures were optimized by using DS. Protein and ligand were prepared for the reverse target and docking simulation by adding partial charges and hydrogen with the aid of DS. The proteins can be acquired from the database of Protein Data Bank (PharmaDB pharmacophores, New York,, NY, USA). Ligand and pharmacophores were matched in DS.

 10.1002/cbdv.201800559

The X-ray crystal structure of NF-κB p65 (PDB 1MY5) complexed with the inhibitor was obtained from the RCSB Protein Data Bank. Vina docking encoded in DS 2017 R2 software was employed to identify the potential binding of 2d to NF-κB p65. Docking parameters were set to default values. All docked poses of 2d were clustered using a tolerance of 2 Å for RMSD and were ranked on the basis of the binding docking energies. The lowest energy conformation in the most populated cluster was selected for subsequent study.

SPR assay

SPR experiments were performed with a Biacore T200 apparatus on CM5 sensor chips (GE Healthcare, Fairfield, CT, USA), following the published protocol [18]. Ligand solutions (at 12.5, 25, 50, 100, 200 and 400 nM.) were prepared with running buffer by serial dilutions from stock solutions. The sensorgrams were analyzed with the Biacore T200 evaluation software (version 2.0, Fairfield, CT, USA). The kinetic parameters, including association rate constants (ka), dissociation rate constants (kd), and kinetic dissociation constant (KD), were calculated by Biacore T200 evaluation software 2.1 (Fairfield, CT, USA).

Western Blot assay

The RAW 264.7 cells were stimulated with LPS (1 μg/mL) for 24 h then treated with various concentrations of the compound **2d** (10 and 20 μM) and Bay 11-7082 (0.3 μg/ml) for 24 h. The samples of total cellular protein extracts were loaded and separated by SDS-PAGE and were transferred on PVDF membranes (Beyotime Biotechnology, Haimen, China). The membranes were blocked with 5% dehydrated skim milk in TBST for 2 hr at room temperature. The blots were washed thrice in TBST buffer and were incubated overnight at 4 °C with primary antibodies against β-actin (1:1000 dilution), NF-κB p65 (1:1000 dilution), iNOS (1:1000 dilution), COX-2 (1:1000 dilution) and phospho NF-κB p65 (1:1000 dilution) (all from Cell Signaling Technology, Inc., Danvers, MA, USA). The blots were washed thrice in TBST buffer, followed by the addition of secondary antibodies. The unbound antibodies in each step were washed with TBST three times. The specific proteins in the blots were visualized using an enhanced chemiluminescence reagent (Thermo Scientific, Waltham, MA, USA). Immunoreactivity of the membranes were detected

using the Bio-Rad-Image Lab with an electrochemiluminescence system (Thermo Fisher Scientific, Waltham, MA, USA). The densitometry of the protein bands was measured using the ImageJ (NIH image software) and was normalized to their relevant controls.

Statistical Analysis

Results are expressed as mean ± standard deviation. Statistical comparisons were performed using one-way ANOVA followed by the least significant difference test. The minimum level of significance was $p < 0.05$.

Acknowledgments

This work was supported by the General Financial Grants from the China Postdoctoral Science Foundation (2015M571916), the National Nature Science Foundation of China (81302701).

Author Contribution Statement

Z. L. designed the work, C. M. contributed to the synthesis and of the compound. C. M. and M. W. evaluation of the biological activity.

Appendix A. Supplementary data

The supplementary data associated with this article can be found in the online version at……..

References

[1] H. Tilg, A.R. Moschen, 'Adipocytokines: mediators linking adipose tissue, inflammation and immunity', *Nat. Rev. Immunol*. **2006**, *6*, 772-783.

[2] G. Siasos, V. Tsigkou, E. Oikonomou, M. Zaromitidou, S. Tsalamandris, K. Mourouzis, M. Vavuranakis, M. Anastasiou, K. Vlasis, M. Limperi, V. Gennimata, J.N. Boletis, A.G. Papavassiliou, D. Tousoulis, 'Circulating Biomarkers Determining Inflammation in Atherosclerosis Progression', *Curr. Med. Chem.* **2015**, *22*, 2619-2635.

[3] K. Kux, C. Pitsouli, 'Tissue communication in regenerative inflammatory signaling: lessons from the fly gut', *Front Cell Infect Microbiol.* **2014**, *4*, 49.

[4] S. Zhang, X. Yang, L. Wang, C. Zhang, 'Interplay between inflammatory tumor microenvironment and cancer stem cells', *Oncol Lett.* **2018**, *16*, 679-686.

[5] L. Zhang, L. Yang, 'Anti-inflammatory effects of vinpocetine in atherosclerosis and ischemic stroke: a review of the literature', *Molecules.* **2014**, *20*, 335-347.

10.1002/cbdv.201800559

[6] S. Görög, 'Advances in the analysis of steroid hormone drugs in pharmaceuticals and environmental samples (2004-2010)', *J. Pharm. Biomed. Anal.* **2011**, *55*, 728-743.

[7] S. Sehajpal, D.N. Prasad, R.K. Singh, 'Prodrugs of Non-steroidal Anti-inflammatory Drugs (NSAIDs): A Long March Towards Synthesis of Safer NSAIDs', *Mini. Rev. Med. Chem.* **2018**, *18*, 1199-1219.

[8] N.B. Karatzas, 'Coumarins, a class of drugs with a unique contribution to medicine: the tale of their discovery', *Hellenic. J. Cardiol.* **2014**, *55*, 89-91.

[9] T.H. Lee, Y.C. Chen, T.L. Hwang, Shu, P,J. Sung, Y.P. Lim, W.L. Kuo, J.J. Chen, 'New coumarins and anti-inflammatory const C.W. ituents from the fruits of Cnidium monnieri', Int. *J. Mol. Sci.* **2014**, *15*, 9566-9578.

[10] G. Kirsch, A.B. Abdelwahab, P. Chaimbault, 'Natural and Synthetic Coumarins with Effects on Inflammation', *Molecules.* **2016**, *21*, E1322.

[11] H.M. Revankar, S.N. Bukhari, G.B. Kumar, H.L. Qin, "Coumarins scaffolds as COX inhibitors", *Bioorg. Chem.* **2017**, *71*, 146-159.

[12] A.L. Huang, Y.L. Zhang, H.W. Ding, B. Li, C. Huang, X.M. Meng, J. Li, 'Design, synthesis and investigation of potential anti-inflammatory activity of O-alkyl and O-benzyl hesperetin derivatives', *Int. Immunopharmacol.* **2018**, *61*, 82-91.

[13] F. Yi, X.L. Tan, X. Yan, H.B. Liu, 'In silico profiling for secondary metabolites from Lepidium meyenii (maca) by the pharmacophore and ligand-shape-based joint approach', *Chin Med.* **2016**, *11*, 42.

[14] N. Li, W.Y. Xin, B.R. Yao, W. Cong, C.H. Wang, G.G. Hou, 'N-phenylsulfonyl-3,5-bis(arylidene)-4-piperidone derivatives as activation NF-κB inhibitors in hepatic carcinoma cell lines', *Eur. J. Med. Chem.* 2018, *155*, 531-544.

[15] I. Pateras, C. Giaginis, C. Tsigris, E. Patsouris, S. Theocharis, 'NF-κB signaling at the crossroads of inflammation and atherogenesis: searching for new therapeutic links', *Expert Opin Ther Targets.* **2014**, *18*, 1089-1101.

[16] P. Viatour, M.P. Merville, V. Bours, A. Chariot, 'Phosphorylation of NF-kappaB and IkappaB proteins: implications in cancer and inflammation', *Trends Biochem. Sci.* **2005**, *30*, 43-52.

[17] N.D. Perkins, 'Integrating cell-signalling pathways with NF-kappaB and IKK function' *Nat Rev. Mol. Cell Biol.* **2007**, *8*, 49-62.

[18] L. Ji, M. Wu, Z. Li, 'Rutacecarpine Inhibits Angiogenesis by Targeting the VEGFR2 and VEGFR2-Mediated Akt/mTOR/p70s6k Signaling Pathway', *Molecules.* **2018**, *23*, pii: E2047.

10.1002/cbdv.201800559

Graphical Illustration